

Advanced Low-Voltage System-in-Package Half-Bridge MOSFET with Added Protection Features

Original

Advanced Low-Voltage System-in-Package Half-Bridge MOSFET with Added Protection Features / Musumeci, S.; Barba, V.; Scrimizzi, F.; Mistretta, C.. - ELETTRONICO. - (2022). (24th European Conference on Power Electronics and Applications, EPE 2022 ECCE Europe deu 2022).

Availability:

This version is available at: 11583/2979982 since: 2023-07-06T16:01:21Z

Publisher:

Institute of Electrical and Electronics Engineers Inc.

Published

DOI:

Terms of use:

This article is made available under terms and conditions as specified in the corresponding bibliographic description in the repository

Publisher copyright

IEEE postprint/Author's Accepted Manuscript

©2022 IEEE. Personal use of this material is permitted. Permission from IEEE must be obtained for all other uses, in any current or future media, including reprinting/republishing this material for advertising or promotional purposes, creating new collecting works, for resale or lists, or reuse of any copyrighted component of this work in other works.

(Article begins on next page)

Experimental Evaluation of a Monolithic Gallium Nitride Devices Solution for Flyback Converter Devoted to Auxiliary Power Supply

Salvatore Musumeci,
Vincenzo Barba, Michele
Pastorelli
POLITECNICO DI TORINO
Corso Duca degli Abruzzi, 24
Turin, Italy
Tel.: +39 0110907127.
E-Mail:
salvatore.musumeci@polito.it,
vincenzo.barba@polito.it
michele.pastorelli@polito.it
URL: <https://www.polito.it/>

F. Scrimizzi, F. Cammarata,
G. Longo
STMICROELECTRONICS
Stradale Primosole, 50
Catania, Italy
Tel.: +39 957404401.
E-Mail:
filippo.scrimizzi@st.com,
federica.cammarata@st.com,
giuseppe.longo@st.com
URL: <https://www.st.com/>

S. Rizzo
UNIVERSITY OF
CATANIA
Piazza Università, 2
Catania, Italy
Tel.: +39 0957307777.
E-Mail:
salvatore.rizzo@unict.it,
URL: <https://www.unict.it/>

Acknowledgements

The paper was partially funded by PRIN Project ISoREC - Innovative Solutions for Renewables in Energy Communities (ISoREC), MINISTRY (MIUR) Project ic 202054TZLF.

Keywords

GaN FET, Flyback, Monolithic Device, System on Chip.

Abstract

The paper deals with an improved high-voltage smart monolithic Gallium Nitride (GaN) Field effect transistor (FET) as a power device integrated with a control circuit and gate driver with protection features. The high energy density and increased switching frequency of the GaN FETs, together with the low voltage control part, allow for the realisation of a DC-DC converter with a reduced size and high performance. In the paper, a Flyback converter based on the monolithic integrated power switch and signal circuits is described and experimentally evaluated to demonstrate the effectiveness of the proposed solution.

Introduction

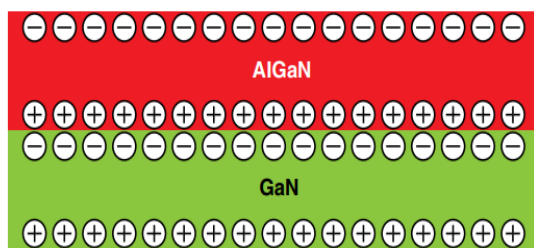
Nowadays, Gallium Nitride (GaN) is probably the most challenging technology in the field of power electronics, allowing the development of high-voltage devices with increased power density, reduced on-resistance, and very high-frequency

switching. The wide band gap of the semiconductor material ($E_g = 3.4$ eV) results in a high critical electric field ($E_c = 3.3$ MV/cm), which can lead to designs of electronic devices with shorter drift region and, therefore, lower on-state resistance when compared to silicon-based one featuring the same voltage rating [1]. The designer's challenge in power device areas is to develop integrated systems to reduce the size and improve reliability. Integrating power electronic components and subsystems such as control, sensors, and driver circuits provides enhanced functionality and improved operating characteristics of the integrated system. In the power electronics field, the System in Package (SiP) is used for the heterogeneous integration of power and control electronic circuits. At the same time, the System on Chip (SoC) is a monolithic solution that implements a power switch and a signal circuit [2]. In industrial or automotive applications, the high-power density and the switching frequencies of High Electron Mobility Transistors (HEMT) such as GaN FET reduce the size and weight of the power board layout compared to the solutions with silicon MOSFET [3]. In the proposed paper, a high voltage (maximum rated voltage $V_{DS}=650V$) GaN FET enhancement lateral device integrated with the control signal circuits and protections in a monolithic solution is described. The monolithic device is implemented for the development of an auxiliary isolated power supply circuit suitable for automotive applications directly connected to the power battery pack (rated voltage 400V) to power the gate driver circuit of a typical Silicon

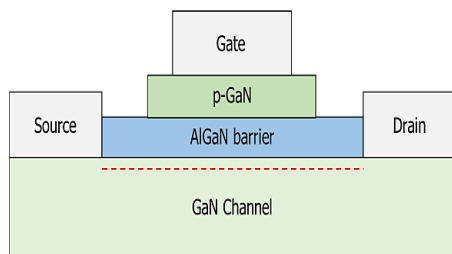
carbide (SiC) MOSFET- based traction inverter [4] or PV inverter interface [5]. The paper presents and discusses a monolithic GaN FET-based Flyback converter system. Several experimental results are carried out to demonstrate the effectiveness of the proposed enhanced integrated device in a laboratory prototype implementation.

Monolithic GaN-based Device Overview

Gallium Nitride devices are based on heterojunction: the interface between two semiconductors (GaN and AlGaN) with dissimilar bandgaps but the same crystal structure. When the AlGaN and GaN layers are grown on top of each other to create the heterojunction, the atoms at the interface are subjected to mechanical stress. This stress will cause a shift of the atoms and, in turn, an electric field with a resulting accumulation of both positive and negative charges on the edges of the layers and thus the creation of Two-Dimensional Electrons Gas (2DEG) [6]. In Fig. 1a, the 2DEG phenomenon is highlighted. By default, Gallium Nitride is a normally-ON technology, but several methods already exist to make it normally off.



a)



b)

Fig. 1: a) 2DEG phenomenon. b) e-mode GaN-based power switch. The normally off effect is obtained by introducing the p-GaN between the p-AlGaN layer and the Schottky Gate.

To use a depletion mode (d-mode) normally on GaN in a power converter, a cascode configuration [7], with a low-voltage MOSFET in series at the GaN source for normally off device switching operation [8] is implemented. This configuration is used for high-current GaN-based power transistors. Direct drive cascode is another alternative to improve the switching device capability. In a direct drive GaN Based switch, the d-mode GaN and the low-voltage MOSFET are driven separately [9].

The cascode solution increases the stray inductances due to using two devices in the same frame. The enhanced mode (e-mode) GaN device is a normally off GaN power transistor with a similar driver circuit like a MOSFET one with a reduced voltage amplitude (5V-6V) [10]. Among the e-mode GaN, intelligent and integrated GaN devices based on p-GaN gate normally off solution is arranged [11]. It is realized by inserting an (Al)GaN layer with p-type doping between the AlGaN barrier and the Schottky gate contact (Fig. 1b). The effect of the introduction of the p-GaN or p-AlGaN layer is an increase in the band diagram with the resulting depletion of the 2DEG even at zero gate bias. Due to this, the AlGaN conduction band results above the Fermi level, so a positive gate bias is needed to induce electrons in the channel under the gate. Based on Gallium Nitride technology, the integrated power device features a 650V maximum rated voltage with 190 mΩ of $R_{DS(on)}$ (at ambient temperature). Both 12V Enhancement HEMTT and 12V Depletion HEMT plus Resistor and P GaN capacitors and 650V N Enhancement HEMT basic technology block are used in the monolithic integrated circuit (IC). The power switch is a lateral enhancement-mode GaN FET with a current sensing cell used for overcurrent detection. The low-voltage HEMT devices and components are used to implement the driver/controller on the same chip assembled in a plastic SO16 package. The block diagram of the integrated device is reported in Fig. 2.

The lateral configuration of GaN-Based devices shows attractive monolithic solutions, such as integrating several circuits and sensing components with simple isolation and shielding among the different parts. Furthermore, the connection of the substrate to the ground and the capability of physical contact with a heat sink allows optimal thermal management. Moreover, the stray inductances of the power loop with the monolithic solution can be reduced by avoiding the dangerous voltage gate and drain ringing

during the switching transients [12]. The power SoC arrangement combines features such as variable current mode PWM controller, soft start, programmable turn-on dv/dt , and thermal diagnostic.

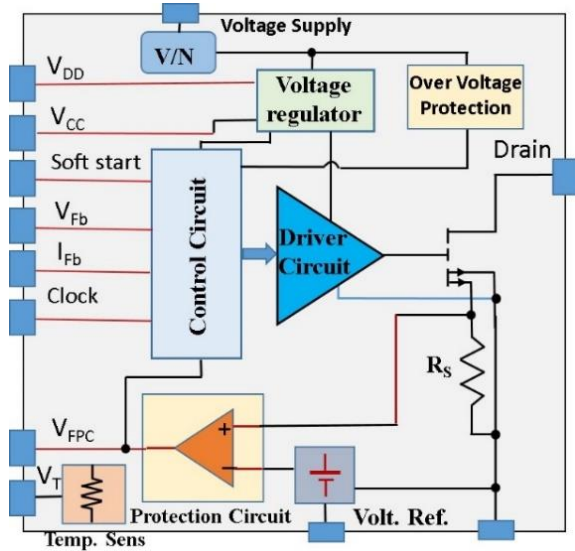


Fig. 2: Block diagram of integrated GaN-based power switch, controller/driver circuit, and protections

Furthermore, the integrated power electronic device includes several protections, such as over temperature, overcurrent, and over voltage. Moreover, electrostatic discharge protection is implemented. The power GaN FET hard switching cycle for the maximum drain current rate ($I_{D,peak}=17A$) at Drain-Source voltage $V_{DS}=500V$ is reported in Fig. 3. The experimental hard switching waveforms are related to a monolithic device with a higher current rate. The device feature described makes it appropriate for Flyback operation, with high flexibility loop regulation parameters adjustable by external settings (resistances and capacitances).

Auxiliary power supply for power converter Circuits

The number of power converters in electric vehicles is high, and the energy density is a crucial point in the technology design approach. Fig. 4 shows an electrical automotive platform for mid-range power with power converters' position and layout. The power converters' size and weight are fundamental in maximising space and vehicle autonomy. High bandgap technologies make it possible to considerably reduce the size

of passive components thanks to the high switching frequencies. GaN devices, in particular, in addition to having high switching frequencies, also show high energy densities and the possibility of integration with increasingly higher control and protection circuits. Auxiliary DC/DC converters are widely used to power the electronic equipment in the vehicle. Furthermore, the inverters for electric propulsion or other applications, such as power steering, air conditioning, etc., request some auxiliary power supply to power the electronic switches, gate driver, and control circuits, etc.

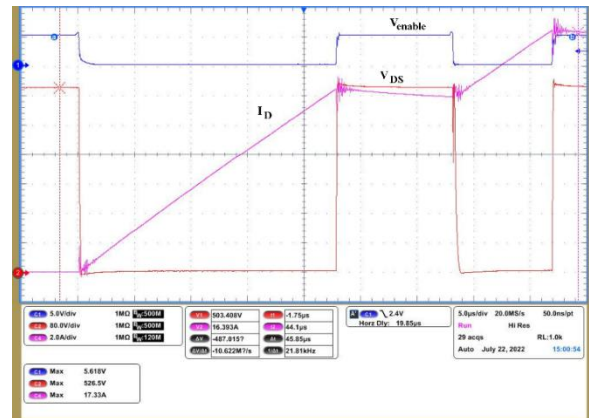


Fig. 3: Inductive switching cycle of the power GaN FET of the monolithic device at the maximum current rate available with the described device technology. Venable is a complementary logic command signal that enables the gate driver circuit. $V_{DS}=80V/div$, $I_D= 2A/div$, $V_g=5V/div$, $t=5ms/div$

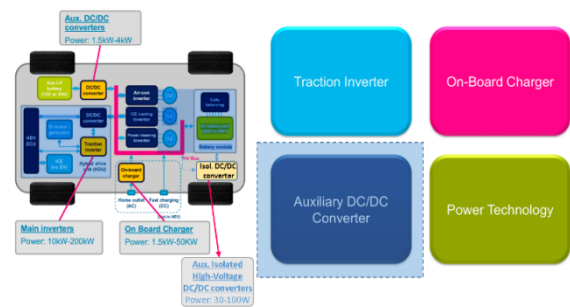


Fig. 4: Block diagram Electric Vehicle (EV) platform with the main power converters classification and location

The auxiliary power supply can be isolated or not isolated depending on the load and safety requirement (see Fig. 4). Generally, the auxiliary DC/DC converters are connected to the low-voltage battery source (12V-48V) [13]. The DC/DC converter can be connected to the high-

The power GaN FET features 650V and a direct resistance, $R_{DS,on}=190m\Omega$.

The power converter can operate in three modes:

- DCM (Discontinuous Current Mode)
- CCM (Continuous Current Mode)
- CrCM (Critical Conduction Mode, boundary between DCM and CCM)

The voltage stress on the drain of the GaN FET is an important parameter for monitoring. In a Flyback circuit, the GaN FET peak voltage is given by

$$V_{DS,peak} = V_{supply} + \frac{N_1}{N_2} \cdot V_{out} + V_{spike} + V_{SM} \quad (1).$$

From which

$$V_{DS,max} > V_{DS,peak} \quad (2).$$

The maximum rate voltage of the GaN FET, $V_{DS,max}$ is related to the V_{supply} and depends on the turn ratio plus the voltage spike due to the stray inductances (V_{spike}) with a safe margin voltage (V_{SM} , a 20% of the maximum GaN FET voltage rate) [15]. To contain voltage under $V_{DS,max}$ RCD snubber circuit is implemented, as shown in Fig. 5.

Experimental test at minimum supply Voltage

Several tests are carried out at a minimum supply voltage of around 200V to ensure the requested output voltage.

The first experimental test shows the waveform I_{out} , V_{DS} , and V_{out} at $I_{load}=2.5A$ and V_{supply} sets at 210V with $V_{out}=14V$.

The waveforms caught in such conditions are in steady-state working mode, as shown in Fig.8a. The switching frequency is stable at 410kHz, and the V_{DS} is well damped (without the intervention of the RCD snubber). The resonance frequency is around 8.6MHz, as shown in Fig. 8b, with a maximum value of $V_{DS,max}=434V$. The operation duty cycle is

$$d = t_{on} \cdot f_{sw} = 600ns \cdot 450kHz = 0.24 \quad (3).$$

The V_{DS} curve shows an operation mode between DCM and CrCM.

At No load, the voltage regulator must guarantee the output voltage requested. The experimental

pictures in Fig 9 show the waveforms I_{out} , V_{DS} , the input current I_{in} , and V_{out} at no load (V_{supply} sets at 245V). In such conditions, the system works in burst mode.

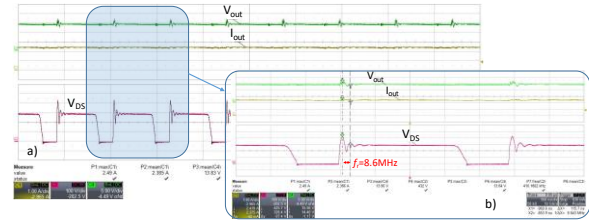


Fig. 8: Switching waveforms of the output electrical quantities and Drain-Source voltage. a) Steady-state operation. b) zoomed view. $V_{DS}=100V/div$, $I_{out}=1A/div$, $V_{out}=5V/div$, a) $t=2\mu s/div$, b) $t=500ns/div$

The V_{out} is stable at 15V in a steady state, and I_{in} is lower (around 3.2mA). The input power dissipation P_{in} is

$$P_{in} = V_{in} \cdot I_{in} = 245V \cdot 3.2mA = 0.78W \quad (4).$$

The $V_{DS,max}$ is 377V.

The V_{DS} pulses sequence alternates with a frequency of 363Hz (from Fig.9a) instead; the pulses have a switching frequency 1.64MHz for 25 μs , as shown in Fig.9b.

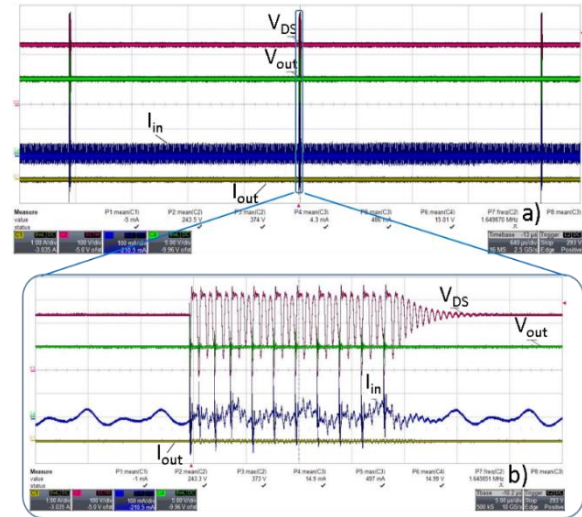


Fig. 9: Switching waveforms of the main electrical quantities in the case of burst mode. a) Steady-state operation. b) zoomed view. $V_{DS}=100V/div$, $I_{out}=1A/div$, $I_{in}=100mA/div$, $V_{out}=5V/div$, a) $t=640\mu s/div$, b) $t=5\mu s/div$

The experimental waveforms to demonstrate the voltage regulation at dynamic load conditions are reported in Fig. 10. V_{supply} was set at 200V, and the dynamic load was set at two different output currents, specifically 1A for 100ms and 2A for

100ms. The Flyback operated in steady state condition, and the output voltage was stable to the value selected. No anomalous working conditions were detected during the tests. The V_{DSmax} is 418V, and the switching frequency was attested at 434kHz; the V_{out} average value measured is 13.87V.

For the experimental prototype built, the maximum efficiency was measured at 84.4% at $I_{out}=2.2A$.

Experimental test at maximum supply Voltage

The experimental tests are carried out at

- $V_{in}=400V$
- $V_{out}=14V$
- $I_{out}=3A$
- $f_{sw}=236kHz$

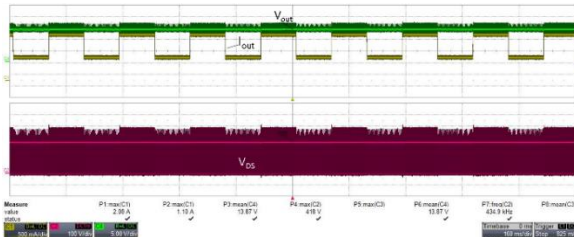


Fig. 10: Switching waveforms at dynamic load variation in steady-state operation. $V_{DS}=100V/div$, $I_{out}=500mA/div$, $V_{out}=5V/div$, $t=160ms/div$

The waveforms show that the system is able to work as a Flyback converter in continuous operation, guaranteeing about 14V at the output and with a load current equal to 3A, with an output power of $P_{out}=42W$.

In those conditions, the GaN FET device is in on state for $t_{on}=387ns$; oscillation peaks characterize the drain-source voltage equal to 680V with a frequency of about 8MHz, while the maximum drain current peak is 2.5A. The switching waveforms of the drain-source voltage and drain current are reported in Fig. 11.

The system is in DCM operation, considering the resonance oscillation on the V_{DS} waveform shown in Fig. 11. The power losses on the GaN FET power switch (P_D) are evaluated in Fig. 12. From the measurements in Fig. 12, the power losses at turn-off are $P_{Doff}=200W$, while at turn-on, $P_{Don}=14W$.

The burst mode operation is depicted in Fig. 13. The Flyback solution is able to follow the burst mode operation when working at zero or light

load $I_{out} < 0.5A$. the current required on the low voltage third wiring (I_{Vcc}) with light load only is about 17mA. In Fig. 13, the voltage related to the clock pin (V_{Clock}) is reported to demonstrate the correct and stable control acting at light load.

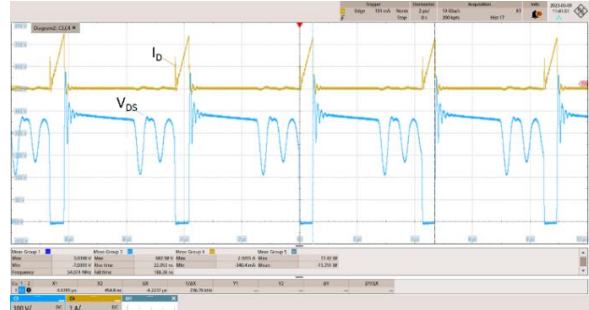


Fig. 11: GaN FET switching waveforms in steady state at $V_{out}=14V$, $I_{out}=3A$. $V_{DS}=100V/div$, $I_D=1A/div$, $t=2\mu s/div$

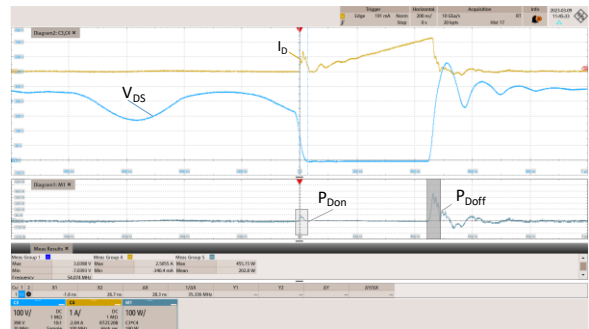


Fig. 12: GaN FET single switching cycle waveforms and power loss (P_D) evaluation at $V_{out}=14V$, $I_{out}=3A$. $V_{DS}=100V/div$, $I_D=1A/div$, $t=200ns/div$

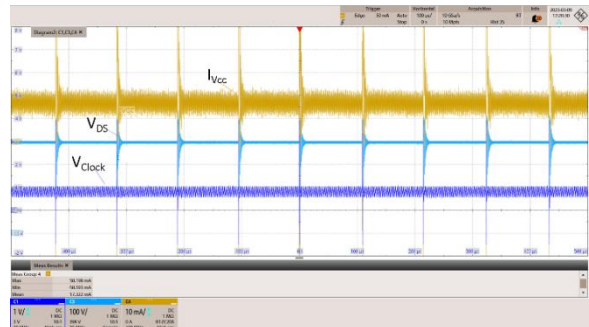


Fig. 13: Switching waveforms of the main electrical quantities in the case of burst mode $V_{out}=14V$, $I_{out}=0.05A$, $V_{DS}=400V$. $V_{out}=100V/div$, $V_{Clock}=1V/div$, $I_{out}=10mA/div$, $t=100\mu s/div$

Finally, in the dynamic load variation (tests from 0 to 1.5A and from 1.5A to 3A), the Flyback regulator is able to follow the current set point modified after 500ns dynamically. The switching waveforms of the step current load variation from

1.5A to 3A and the output voltage regulation are reported in Fig. 14.

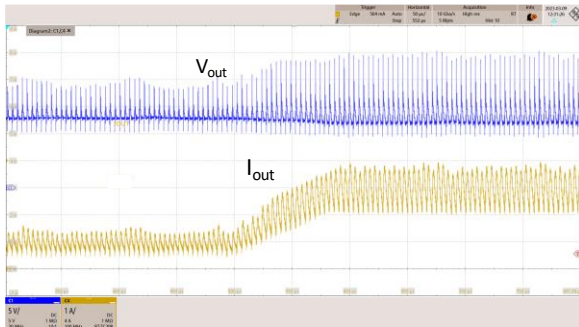


Fig. 14: Flyback output voltage regulation for a step load Dynamic load variation 1.5A to 3A. $V_{out}=14V$, $I_{out}=3A$. $V_{out}=5V/div$, $I_{out}=1A/div$, $t=50\mu s/div$

Conclusion

In the paper, a last generation of a monolithic GaN power device with an integrated control/driver circuit and protections devoted to a Flyback converter arrangement is described and experimentally evaluated. The high switching frequency obtainable with the HEMT devices and the integration capability allows a compact and effective high-voltage power Flyback converter appropriate for an auxiliary power supply connected to a 400V battery source. The power converter obtained may be used to power the several low-voltage electronic circuits of an inverter or auxiliary DC-DC converter, typically of propulsion system applications

References

- [1]. Kaminski N. Hilt O.: SiC and GaN devices – wide bandgap is not all the same, Volume8, Issue3, Special Issue: Power Semiconductor Devices and Integrated Circuit, May 2014, Pages 227-236, doi: <https://doi.org/10.1049/iet-cds.2013.0223>
- [2]. Pendharkar S.: Smart power technologies enabling power SOC and SIP, 2016 IEEE Symposium on VLSI Technology, Honolulu, HI, USA, 14-16 June 2016, Honolulu, HI, USA, pp. 1-2, doi: 10.1109/VLSIT.2016.7573394
- [3]. Yuruk H. Keysan O. Ulutas B.: Comparison of the Effects of Nonlinearities for Si MOSFET and GaN E-HEMT Based VSIs, in IEEE Transactions on Industrial Electronics, vol. 68, no. 7, pp. 5606-5615, July 2021, doi: 10.1109/TIE.2020.2996132
- [4]. Gao R. Yang Yu L. W. Husain I.: Gate driver design for a high power density EV/HEV traction drive using silicon carbide MOSFET six-pack power modules, 2017 IEEE Energy Conversion Congress and Exposition (ECCE), Cincinnati, OH, USA, 2017, pp. 2546-2551, doi: 10.1109/ECCE.2017.8096484.
- [5]. Qureshi, M. A. et al.: "A Novel Adaptive Control Approach for Maximum Power-Point Tracking in Photovoltaic Systems," Energies, 2023 16(6), 2782. <https://doi.org/10.3390/en16062782>
- [6]. Lidow A. De Rooij M. Strydom J. Reusch D. Glaser J.: GaN Transistors for Efficient Power Conversion, 3rd ed.; John Wiley & Sons: Hoboken, NJ, USA, 2019.
- [7]. Xu, J. et al.: Cascode GaN/SiC: A Wide-Bandgap Heterogenous Power Device for High-Frequency Applications, in IEEE Transactions on Power Electronics, vol. 35, no. 6, pp. 6340-6349, June 2020, doi: 10.1109/TPEL.2019.2954322
- [8]. Buonomo S. et al.: Driving a New Monolithic Cascode Device in a DC-DC Converter Application, in IEEE Transactions on Industrial Electronics, vol. 55, no. 6, pp. 2439-2449, June 2008, doi: 10.1109/TIE.2008.921655.
- [9]. Sugiyama T. et al.: Stable cascode GaN HEMT operation by direct gate drive," 2020 32nd International Symposium on Power Semiconductor Devices and ICs (ISPSD), Vienna, Austria, 2020, pp. 22-25, doi: 10.1109/ISPSD46842.2020.9170130.
- [10]. Musumeci S. Barba. V.: Gallium Nitride Power Devices in Power Electronics Applications: State of Art and Perspectives, (2023) Energies, 16(9), 3894. <https://doi.org/10.3390/en16093894>
- [11]. Musumeci S. Armando E. Mandrile F. Scrimizzi F. Longo G. Mistretta C.: Experimental Evaluation of an Enhanced GaN-Based Non-Symmetric Switching Leg Integrated Module for Synchronous Buck Converter Applications, 2021 23rd European Conference on Power Electronics and Applications (EPE'21 ECCE Europe), Ghent, Belgium, 2021, pp. 1-10, doi: 10.23919/EPE21ECCEurope50061.2021.9570541.
- [12]. Zhu L. Bai H. Brown A. McAmmond M.: Design a 400 V-12 V 6 kW Bidirectional Auxiliary Power Module for Electric or Autonomous Vehicles With Fast Precharge

Dynamics and Zero DC-Bias Current, in IEEE Transactions on Power Electronics, vol. 36, no. 5, pp. 5323-5335, May 2021, doi: 10.1109/TPEL.2020.3028361

- [13]. Scrimizzi F. et al.: The GaN Breakthrough for Sustainable and Cost-Effective Mobility Electrification and Digitalization. Electronics 2023, 12, 1436. <https://doi.org/10.3390/electronics12061436>
- [14]. Musumeci S. Stella F. Mandrile F. Armando E. Fratta A.: Soft-Switching Full-Bridge Topology with AC Distribution Solution in Power Converters' Auxiliary Power Supplies, Electronics 2022, 11(6), 884; <https://doi.org/10.3390/electronics11060884>
- [15]. Papanikolaou N. P. Tatakis E. C.: Active voltage clamp in flyback converters operating in CCM mode under wide load variation, in IEEE Transactions on Industrial Electronics, vol. 51, no. 3, pp. 632-640, June 2004, doi: 10.1109/TIE.2004.825342